

A REDUCED ORDER APPROACH FOR THE EMBEDDED SHIFTED BOUNDARY FEM AND A HEAT EXCHANGE SYSTEM ON PARAMETRIZED GEOMETRIES

E.N. KARATZAS^{1,*}, G. STABILE¹, N. ATALLAH², G. SCOVAZZI², AND G. ROZZA¹

ABSTRACT. A model order reduction technique is combined with an embedded boundary finite element method with a POD-Galerkin strategy. The proposed methodology is applied to parametrized heat transfer problems and we rely on a sufficiently refined shape-regular background mesh to account for parametrized geometries. In particular, the employed embedded boundary element method is the Shifted Boundary Method (SBM), recently proposed in [17]. This approach is based on the idea of shifting the location of true boundary conditions to a surrogate boundary, with the goal of avoiding cut cells near the boundary of the computational domain. This combination of methodologies has multiple advantages. In the first place, since the Shifted Boundary Method always relies on the same background mesh, there is no need to update the discretized parametric domain. Secondly, we avoid the treatment of cut cell elements, which usually need particular attention. Thirdly, since the whole background mesh is considered in the reduced basis construction, the SBM allows for a smooth transition of the reduced modes across the immersed domain boundary. The performances of the method are verified in two dimensional heat transfer numerical examples.

1. INTRODUCTION

In this work we present a reduced order modeling strategy for parametrized geometries, starting from an embedded boundary method solver. The main idea in the current manuscript is to exploit the advantages of embedded methods and in particular of the Shifted Boundary Method (SBM), [17, 18, 25], in a reduced order modeling setting. Embedded methods, as full order conformal finite element methods, discretize the original set of equations into a usually high dimensional system of algebraic equations. When a large number of different system configurations need to be tested, or a large reduction in computational cost is the goal, the resolution of such high dimensional system of equations becomes unfeasible. Reduced Order Methods (ROM) have demonstrated to be a viable way to limit the computational burden [12, 19, 6, 4]. In this particular case, the attention is focused on parametrized geometries. The methodology is tested on a simple heat transfer problem which will serve as a base for future more complex scenarios such as flow problems [15]. The manuscript is organized as follows: in Section 2 we introduce the mathematical problem and its full order discretization; in Section 3 we present the reduced order model formulation and its main features and differences with respect to a standard setting; finally in Section 4 numerical results are reported, and in Section 5 conclusions and perspectives for future improvements are given.

¹SISSA, INTERNATIONAL SCHOOL FOR ADVANCED STUDIES, MATHEMATICS AREA, MATHLAB TRIESTE, ITALY.

²CIVIL AND ENVIRONMENTAL ENGINEERING, DUKE UNIVERSITY, DURHAM, NC 27708, UNITED STATES.

E-mail addresses: efthymios.karatzas@sisssa.it, gstable@sisssa.it, nabil.atallah@duke.edu, guglielmo.scovazzi@duke.edu, grozza@sisssa.it.

*Corresponding Author.

2. FULL ORDER MODEL APPROXIMATION

We start recalling, by a sketch description, the continuous strong formulation of the problem and the weak formulation used for the full-order discretization of the problems under consideration. The discrete SBM formulation will be used for the Full Order Method (FOM) simulation during the offline stage. The ROM is constructed using a Proper Orthogonal Decomposition (POD) Galerkin approach following what is reported in Section 3.

2.1. The Thermal-Heat exchange model. Given a k -dimensional parameter space \mathcal{P} and the parameter vector $\mu \in \mathcal{P} \subset \mathbb{R}^k$, let $\mathcal{D}(\mu) \subset \mathbb{R}^d$, $d = 2, 3$ be a bounded parametrized domain depending on μ , with boundary $\Gamma(\mu)$. We consider the following model problem in $\mathcal{D}(\mu)$:

Find the temperature $T(\mu) : \bar{\mathcal{D}}(\mu) \times \mathcal{P} \rightarrow \mathbb{R}^d$ such that in \mathcal{P} we have

$$(1) \quad \begin{aligned} -\Delta T(\mu) &= f(\mu) && \text{in } \mathcal{D}(\mu), \\ T(\mu) &= g_D(\mu) && \text{on } \Gamma_D(\mu), \end{aligned}$$

where $\Gamma_D(\mu)$ is the boundary onto which a Dirichlet boundary condition is applied, and the imposed forces $f(\mu)$, $g_D(\mu)$ are given functions in $\mathcal{D}(\mu)$ and on the boundary $\Gamma_D(\mu)$, respectively.

2.2. Weak SBM formulation. In this subsection we briefly recall the SBM formulation which was originally presented in [17, 18, 25]. In what follows, we denote by $\tilde{\Gamma}$ the surrogate boundary composed of the edges/faces of the mesh that are the closest to the true boundary Γ . The closest faces/edges of $\tilde{\Gamma}$ to Γ are detected by means of a closest-point projection algorithm.

The surrogate boundary $\tilde{\Gamma}$ encloses the surrogate domain $\tilde{\mathcal{D}}$. Furthermore, $\tilde{\mathbf{n}}$ indicates the unit outward-pointing normal to the surrogate boundary $\tilde{\Gamma}$, and it differs from the outward-pointing normal \mathbf{n} of Γ (see Figure 1).

Notice also that the closest-point projection, in spite of the segmented/faceted nature of the surrogate boundary $\tilde{\Gamma}$ is actually a smooth mapping \mathbf{M} from points \tilde{x} on $\tilde{\Gamma}$ to points x on Γ , namely,

$$\mathbf{M} : \tilde{\mathbf{x}}|_{\tilde{\Gamma}} \rightarrow \mathbf{x}|_{\Gamma},$$

which also defines a distance vector function:

$$\mathbf{d} \equiv \mathbf{d}_{\mathbf{M}}(\tilde{\mathbf{x}}) = \mathbf{x} - \tilde{\mathbf{x}} = [\mathbf{M} - \mathbf{I}](\tilde{\mathbf{x}}).$$

The distance vector, as seen in Figure 1, is oriented along the normal to the true boundary, that is $\mathbf{d} = \|\mathbf{d}\|\mathbf{n}$, as a consequence of the use of the closest point projection. Between the normal \mathbf{n} to the true boundary and the normal $\tilde{\mathbf{n}}$ to the surrogate boundary, the minimal grid resolution assumption $\mathbf{n} \cdot \tilde{\mathbf{n}} \geq \mathbf{0}$ is made. The unit normal vector \mathbf{n} and the unit tangential vectors $\boldsymbol{\tau}_i$ ($1 < i < d-1$) to the boundary Γ , can be easily extended to the boundary $\tilde{\Gamma}$ since $\bar{\mathbf{n}}(\tilde{\mathbf{x}}) \equiv \mathbf{n}(\mathbf{M}(\tilde{\mathbf{x}}))$, $\bar{\boldsymbol{\tau}}_i(\tilde{\mathbf{x}}) \equiv \boldsymbol{\tau}_i(\mathbf{M}(\tilde{\mathbf{x}}))$. Here we denote by $\bar{\mathbf{n}}$, $\bar{\boldsymbol{\theta}}_i$ the extensions to $\tilde{\Gamma}$ of \mathbf{n} , $\boldsymbol{\tau}_i$, which are defined on Γ . In the following, whenever we write $\mathbf{n}(\tilde{\mathbf{x}})$ we actually mean $\bar{\mathbf{n}}(\tilde{\mathbf{x}})$ at a point $\tilde{\mathbf{x}} \in \tilde{\Gamma}$, and similarly for $\boldsymbol{\tau}_i(\tilde{\mathbf{x}})$ and $\bar{\boldsymbol{\theta}}_i(\tilde{\mathbf{x}})$. Moreover, the above constructions are the key ingredients when building an extension \bar{g}_D of the Dirichlet boundary condition g_D to the boundary $\tilde{\Gamma}$ of the surrogate domain.

Now we can introduce the Shifted Boundary (SB) variational formulation. The SBM weak discrete formulation for the heat exchange system, with non-homogeneous Dirichlet boundary conditions, reads:

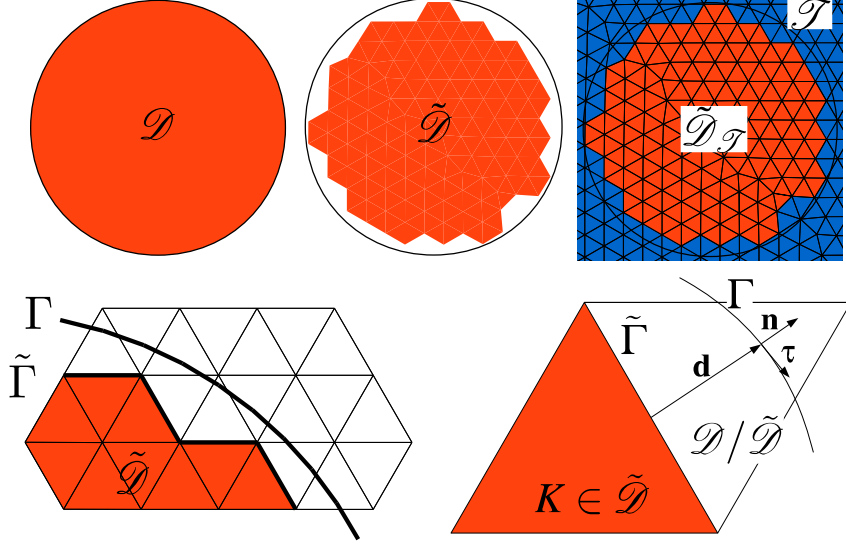


FIGURE 1. Example of the SBM mesh on a disc. In the first row, from left to the right: the real geometry; the SBM surrogate geometry and the background mesh together with the surrogate SBM discretized geometry. In the second row, from left to the right: a zoom of the surrogate SBM mesh/ surrogate boundary and the normal and distance vector considering one element.

Find $T \in V_h = \left\{ v \in C^0(\tilde{\mathcal{D}}(\mu)) : v|_K \in P^1(K), \forall K \in \tilde{\mathcal{D}}_{\mathcal{T}}(\mu) \right\}$, with number of degrees of freedom equal to $\dim V_h = N_h < \infty$ for all $h > 0$ such that

$$(2) \quad a(T, w) = \ell(w), \quad \forall w \in V_h,$$

with

$$\begin{aligned} a(T, w) &= (\nabla w, \nabla T)_{\tilde{\mathcal{D}}} - \langle w + \nabla w \cdot \mathbf{d}, \nabla T \cdot \tilde{\mathbf{n}} \rangle_{\tilde{\Gamma}_D} - \langle \nabla w \cdot \tilde{\mathbf{n}}, T + \nabla T \cdot \mathbf{d} \rangle_{\tilde{\Gamma}_D} \\ &\quad + \langle \nabla w \cdot \mathbf{d}, (\mathbf{n} \cdot \tilde{\mathbf{n}}) / \|\mathbf{d}\| \nabla T \cdot \mathbf{d} \rangle_{\tilde{\Gamma}_D} + \langle \alpha / h^\perp (w + \nabla w \cdot \mathbf{d}), T + \nabla T \cdot \mathbf{d} \rangle_{\tilde{\Gamma}_D}, \\ \ell(w) &= (w, f)_{\tilde{\mathcal{D}}} - \langle \nabla w \cdot \tilde{\mathbf{n}}, \bar{g}_D \rangle_{\tilde{\Gamma}_D} - \langle \nabla w \cdot \mathbf{d}, (\nabla \bar{g}_D \cdot \boldsymbol{\tau}_i) \boldsymbol{\tau}_i \cdot \tilde{\mathbf{n}} \rangle_{\tilde{\Gamma}_D} \\ &\quad + \langle \alpha / h^\perp (w + \nabla w \cdot \mathbf{d}), \bar{g}_D \rangle_{\tilde{\Gamma}_D}, \end{aligned}$$

where α is the Nitsche penalty parameter, h^\perp is a characteristic length of the elements in the direction orthogonal to the boundary and \mathbf{d} , \mathcal{T} , $\tilde{\mathcal{D}}_{\mathcal{T}}$ are the distance vector, the background mesh and the discretized surrogate geometry respectively, see e.g Figure 1. Finally, the standard notation $(\cdot, \cdot)_{\tilde{\mathcal{D}}}$, $\langle \cdot, \cdot \rangle_{\tilde{\Gamma}_D}$ have been used for the $L^2(\tilde{\mathcal{D}})$ and $L^2(\tilde{\Gamma}_D)$ inner products onto the surrogate geometry $\tilde{\mathcal{D}}$ and $\tilde{\Gamma}_D$, respectively.

The idea of the Shifted Boundary method is to enforce the Dirichlet boundary conditions weakly on the surrogate domain and to modify the value of the boundary conditions to be imposed by means of a second-order accurate Taylor expansion, that is $T + \nabla T \cdot \mathbf{d} \approx \bar{g}_D$, with the purpose of maintaining overall second-order accuracy with a piecewise linear discretization.

The SBM weak formulation can be transformed in a system of linear equations and rewritten in matrix form:

$$(3) \quad \mathbf{A}(\mu) \mathbf{T}(\mu) = \mathbf{F}_g(\mu),$$

where $\mathbf{A}(\mu) \in \mathbb{R}^{N_h \times N_h}$ corresponds to the bilinear form $a(\cdot, \cdot)$, $\mathbf{T}(\mu) \in \mathbb{R}^{N_h \times 1}$ is the vector of the unknowns and $\mathbf{F}_g(\mu) \in \mathbb{R}^{N_h \times 1}$ corresponds to the linear form $\ell(\cdot)$.

3. REDUCED ORDER METHOD BY A POD-GALERKIN TECHNIQUE

In this section we briefly recall the POD-Galerkin technique used to generate the reduced order model and we highlight its peculiarities with respect to standard approaches. In general a ROM is a simplification of a FOM that preserves essential behavior and dominant effects, for the purpose of reducing solution time or storage capacity. In particular here we employ a projection-based reduced order model which consists of the projection of the governing equations onto the reduced basis space.

In the recent past, RB methods were applied to linear elliptic equations in [21], to linear parabolic equations in [10] and to non-linear problems in [26, 9]. Although the number of works on reduced order models is now considerable (see e.g. [12] and references therein), to the best of the authors' knowledge, only very few research works [1] can be found dealing with embedded boundary methods and ROM.

From a reduced order modeling point of view, our aim is to investigate how ROMs are applied to the SBM and, more generally, to embedded boundary methods. Our main interest is to generate ROMs on parametrized geometries. The SBM unfitted/surrogate mesh finite element method is used to apply parametrization and reduced order techniques considering Dirichlet boundary conditions.

An important objective is also to test the efficiency of a geometrically parametrized reduced order method without the usage of the transformation to reference domains, which can be an important advantage of embedded methods relying on fixed background meshes.

Before going into the details, we just remind the basics of the reduced basis method. The first step is the generation of a set of full order solutions of the parametrized problem under the variation of the parameter values. The final goal of RB methods is to approximate any member of this solution set with a low number of basis functions and is based on a two stage procedure, the offline and the online stage, [19, 23, 11].

Offline stage. In this stage one performs a certain number of full order solves in order to use the solutions for the construction of a low dimensional reduced basis that approximates any member of the solution set to a prescribed accuracy. It is then possible to perform a Galerkin projection of the full order differential operators, describing the governing equations, onto the reduced basis space in order to create a reduced system of equations. This operation usually involves the solution of a possibly large number of high dimensional problems and the manipulation of high-dimensional structures. The required computational cost is high and therefore this operation is usually performed on a high performance system such as a computer cluster.

Online stage. During this stage, that can be performed also on a system with a reduced computational power and storage capacity, the reduced system of equations can be solved for any new value of the input parameters. This offline-online splitting is effective in many scenarios, such as uncertainty quantification, optimization, real-time control, etc, [4, 6].

3.1. POD. In order to generate the reduced basis space, necessary for the projection of the governing equations, one can find in the literature several techniques such as the POD, the Proper Generalized Decomposition (PGD) and the Reduced Basis (RB) with a greedy sampling strategy. For more details about the different strategies, the reader may see [21, 13, 7, 8]. We apply here a POD strategy using the method of snapshots

[24]. In order to assemble the snapshots matrix, the full-order model is solved for each $\mu \in \mathcal{K} = \{\mu^1, \dots, \mu^{N_s}\} \subset \mathbb{R}^k$ where \mathcal{K} is a finite dimensional training set of parameters chosen inside the parameter space \mathcal{P} and k is the size of the vector μ . The number of snapshots is denoted by N_s and the number of degrees of freedom for the discrete full order solution by N_h . The snapshots matrix \mathcal{S} , is then given by N_s full-order snapshots:

$$(4) \quad \mathcal{S} = [T(\mu^1), \dots, T(\mu^{N_s})] \in \mathbb{R}^{N_h \times N_s}.$$

Given a general scalar function $T : \mathcal{D} \rightarrow \mathbb{R}^d$, with a certain number of realizations T_1, \dots, T_{N_s} , and denoting by $(\cdot, \cdot)_{\mathcal{D}}$ and $\|\cdot\|_{L^2(\mathcal{D})}$ the $L^2(\mathcal{D})$ inner product and norm onto the geometry \mathcal{D} , the POD problem consists of finding, for each value of the dimension of POD space $N_{POD} = 1, \dots, N_s$, the scalar coefficients $a_1^1, \dots, a_1^{N_s}, \dots, a_{N_s}^1, \dots, a_{N_s}^{N_s}$ and functions $\varphi_1, \dots, \varphi_{N_s}$ that minimize the quantity:

$$(5) \quad E_{N_{POD}} = \sum_{i=1}^{N_s} \|T_i - \sum_{k=1}^{N_{POD}} a_i^k \varphi_k\|_{L^2(\mathcal{D})}^2, \quad \forall N_{POD} = 1, \dots, N$$

with $(\varphi_i, \varphi_j)_{\mathcal{D}} = \delta_{ij}, \quad \forall i, j = 1, \dots, N_s.$

It can be shown [16] that the minimization problem of equation (5) is equivalent of solving the following eigenvalue problem:

$$\mathbf{C}\mathbf{Q} = \mathbf{Q}\boldsymbol{\lambda}, \quad \text{for } C_{ij} = (T_i, T_j)_{\mathcal{D}}, \quad i, j = 1, \dots, N_s,$$

where \mathbf{C} is the correlation matrix obtained starting from the snapshots \mathcal{S} , \mathbf{Q} is a square matrix of eigenvectors and $\boldsymbol{\lambda}$ is a diagonal matrix of eigenvalues.

The basis functions can then be obtained with:

$$(6) \quad \varphi_i = \frac{1}{N_s \lambda_{ii}^{1/2}} \sum_{j=1}^{N_s} T_j Q_{ij}.$$

The POD space are constructed using the aforementioned methodology resulting in the space:

$$(7) \quad \mathbf{L} = [\varphi_1, \dots, \varphi_{N^r}] \in \mathbb{R}^{N_h \times N^r},$$

where $N^r < N_s$ is chosen according to the eigenvalue decay of $\boldsymbol{\lambda}$, see for example [21, 4].

3.2. Main differences with respect to a reference domain approach. We highlight here that using an embedded approach there is no need to map all the parametrized geometries to a common reference domain as usually done in the reduced order modeling community [23, 20, 2, 22, 21, 4]. The linear and bilinear forms of equation (2), rewritten in a reference domain setting and in a conformal classical finite element method formulation with homogeneous Dirichlet boundary conditions, are transformed into:

$$\begin{aligned} \tilde{a}(w, T; \mu) &= \tilde{\ell}(w; \mu), \\ \tilde{a}(w, T; \mu) &= \int_{\mathcal{D}^*} \nabla w (J_T(\mu))^{-1} (J_T(\mu))^{-T} |J_T(\mu)| \nabla T dx, \\ \tilde{\ell}(w; \mu) &= \int_{\mathcal{D}^*} |J_T(\mu)| f w dx, \end{aligned}$$

where for a reference domain configuration \mathcal{D}^* , $J_T(\mu)$ and $|J_T(\mu)|$ are the Jacobian of the transformation map $\mathcal{T}_{\mathcal{M}}(\mu) : \mathcal{D}^* \rightarrow \mathcal{D}(\mu)$ and its determinants respectively. For simple geometrical parametrizations, it is possible to find an affine decomposition of the map and therefore of the differential operator ensuring a complete splitting between the offline and the online procedure, see e.g. [12]. For more complex cases such an operation

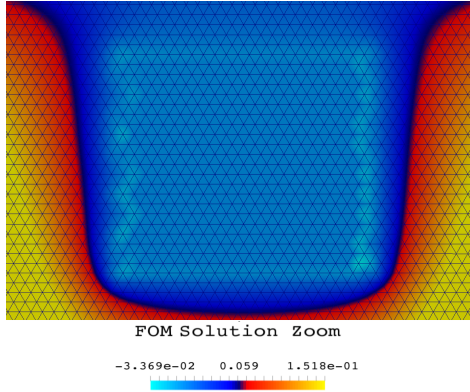


FIGURE 2. A zoom into the embedded rectangle in order to show the smoothing procedure employed by the SBM method inside the ghost area.

becomes not trivial and therefore, in order to ensure an efficient splitting one has to rely on empirical interpolation techniques or similar methods, [3, 5, 20]. In the proposed method, even though an efficient splitting is not trivial, there is no need to rely on a transformation map.

All the solutions are in fact referred to a common background mesh and therefore the projection step and the reduced basis generation become straightforward. Each snapshot however has an “out-of-interest” region which lives inside the embedded domain and that is usually referred as “ghost area”. The location of such part of the domain depends on the parameter μ but the value assumed by the nodes inside that area is arbitrary. The shifted boundary method used herein has the particular advantage that the solution smoothly decreases to zero from the boundary to the interior of the ghost area (see Figure 2). Besides the closest points, where we have such smooth decrease, the value inside the ghost area is set to zero. Since this choice is arbitrary, other choices are also possible (see [14] for more details). Using such an approach we remark that it is usually not possible to easily recover an affine decomposition of the differential operator with respect to the geometrical parameters. However, as highlighted in the next section, it is still possible to rely on hyper reduction techniques, [27, 3, 5].

3.3. The projection stage and the generation of the ROM. Once the POD functional space is set, the reduced field can be approximated with:

$$(8) \quad T^r \approx \sum_{i=1}^{N^r} a_i(\mu) \varphi_i(\mathbf{x}) = \mathbf{L} \mathbf{a}(\mu),$$

where the reduced solution vectors $\mathbf{a} \in \mathbb{R}^{N^r \times 1}$ depend only on the parameter values and the basis functions φ_i depend only on the physical space. The unknown vector of coefficients \mathbf{a} can then be obtained through a Galerkin projection of the full order system of equations onto the POD reduced basis space and with the resolution of a consequent reduced algebraic system:

$$(9) \quad \mathbf{L}^T \mathbf{A}(\mu) \mathbf{L} \mathbf{a}(\mu) = \mathbf{L}^T \mathbf{F}(\mu),$$

which leads to the following algebraic reduced system:

$$(10) \quad \mathbf{A}^r(\mu) \mathbf{a}(\mu) = \mathbf{F}^r(\mu),$$

where $\mathbf{A}^r(\mu) \in \mathbb{R}^{N^r \times N^r}$, and $\mathbf{F}^r(\mu) \in \mathbb{R}^{N^r \times 1}$ are the reduced discretized operators and reduced forcing vector respectively. The dimension of the reduced operator, as seen also in the numerical examples, is usually much smaller than the dimension of the full

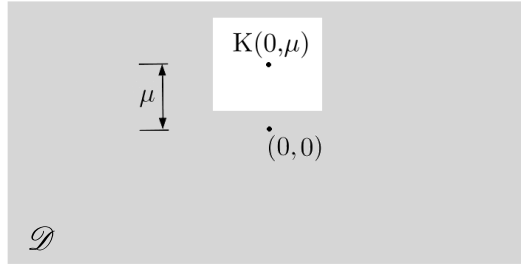


FIGURE 3. Background and embedded geometry for a moving rectangle where the y -coordinate of its baricenter has been parametrized.

order system of equations and therefore much faster to solve. We remark here that the full order discretized differential operators that appear in equation (3) are parameter dependent and therefore, also at the reduced order level, in order to compute the reduced differential operator, we need to assemble the full order operators. Possible ways to avoid such potentially expensive operation, relying on an affine approximation of the full order differential operator, could be to use hyper reduction techniques. In this work, since the attention is mainly devoted to the methodological development of a reduced order method in an embedded boundary setting, rather than in its efficiency, we do not rely on such hyper reduction techniques and we assemble the full order differential operators also during the online stage. Considering that the most demanding computational effort is spent during the resolution of the full order problem rather than in the assembly of the differential operators, as reported in Section 4, it is anyway possible to achieve a computational speedup, and the related results are reported in the next section.

4. NUMERICAL EXPERIMENTS

We consider a parameter space \mathcal{P} and parameter vector $\mu \in \mathcal{P} \subset \mathbb{R}$. Let $\mathcal{D}(\mu) \subset \mathbb{R}^2$, be a bounded parametrized domain depending on μ , with boundary $\Gamma_D(\mu)$. In this Section, we report numerical results for the model problem: Find the reduced basis temperature $T(\mu) : \bar{\mathcal{D}}(\mu) \times \mathcal{P} \rightarrow \mathbb{R}$ such that in \mathcal{P} we have

$$\begin{aligned} -\Delta T(\mu) &= f(\mu) & \text{in } \mathcal{D}(\mu), \\ T(\mu) &= g_D(\mu) & \text{on } \Gamma_D(\mu), \end{aligned}$$

where $\Gamma_D(\mu)$ is the embedded boundary onto which a Dirichlet boundary condition is applied, and the imposed forces $f(\mu)=1$, $g_D(\mu) = 0$ are forcing data in $\mathcal{D}(\mu)$ and on $\Gamma_D(\mu)$, respectively. Two different geometries and parameterizations on an embedded rectangle will be examined. In the first example the y -coordinate of the embedded domain center is parametrized, and in the second one its aspect ratio is considered as a parameter.

4.1. Embedded rectangle with parameterized center. In this first experiment the embedded domain consists of a rectangle of size 0.8×0.7 and its position inside the domain is parametrized with a geometrical parameter μ which describes the position of the rectangle embedded domain with respect to its y -center as in Figure 3.

The horizontal coordinate of the center of the box is not parametrized and is located in the x -center of the domain. The ROM has been trained with 100 and 400 samples for $\mu \in [-0.5, 0.5]$ chosen randomly inside the parameter space. To test the accuracy of the ROM we compared its results on 50 additional samples that were not used to

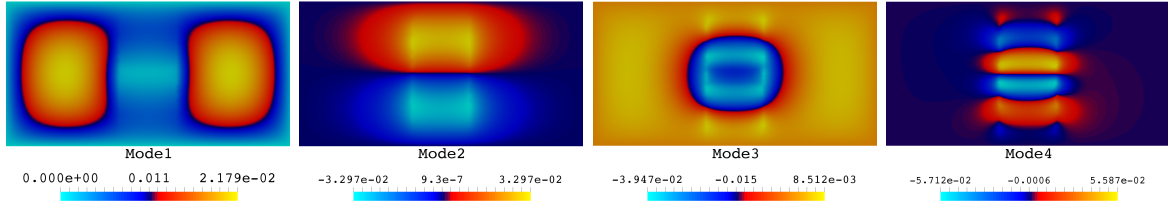


FIGURE 4. The first four basis components with $\mu \in [-0.5, 0.5]$ using 100 snapshots in the offline stage.

TABLE 1. Relative error between the full order solution and the reduced basis solution. Results are reported for different dimensions of the reduced basis space and for fifty test samples.

Num of modes	L^2 proj. ^b	Galerkin proj. ^b	Galerkin proj. ^a
2	6.45035e-02	7.10916e-01	6.95126e-01
5	1.14329e-02	1.44949e-01	1.36034e-01
10	4.83332e-03	2.64459e-02	2.43322e-02
20	2.19454e-03	5.61736e-03	7.45415e-03
30	1.27046e-03	3.30372e-03	4.47413e-03
40	7.72326e-04	2.50189e-03	3.08036e-03
50	5.39532e-04	1.69903e-03	2.39470e-03
100	6.79464e-05	3.36531e-04	1.19915e-03
200	6.40774e-06	1.21062e-04	–
300	3.29000e-06	6.94726e-05	–

^a 100 snapshots, ^b 400 snapshots

create the ROM and were selected randomly within the same range. The background domain size is a rectangle of size $[-2, 2] \times [-1, 1]$ discretized with mesh size $h = 0.035$, while the background mesh boundary is handled as a wall having zero temperature.

In Figure 4, we plot the first four modes obtained with the POD procedure. In Figure 6, we plot the full order solution, the reduced solution and the error for the scalar geometrical parametrized heat equation problem and it is possible to notice that the full and the reduced solution are qualitatively indistinguishable. To verify the behavior of the ROM and its sensitivity with respect to the number of modes in Figure 5 (i) we compare, for different number of modes, the average of the L^2 norm relative error for the 50 different samples used to test the ROM. The plot is reported for both the simple L^2 projection of the full order results on the POD basis functions, and for the ROM results.

Some Comments. In Table 1, for different dimensions of the reduced basis space, we report the relative error of the L^2 Galerkin projection of the snapshots onto the reduced basis space and the relative error of the ROM solution. Two different ROM solutions are examined, using 100 and 400 snapshots during the POD procedure. The plots of Figure 5 (i) are generated with the ROM constructed using 100 and 400 snapshots and the ROM, as well as the L^2 projection, have been tested using 50 different parameter values not previously used to train the ROM.

In Table 2, we report the computational time comparison using different dimensions of the reduced basis space. Even for the case which employs 300 modes (the one with the largest number of modes) we still observe a good computational speedup.

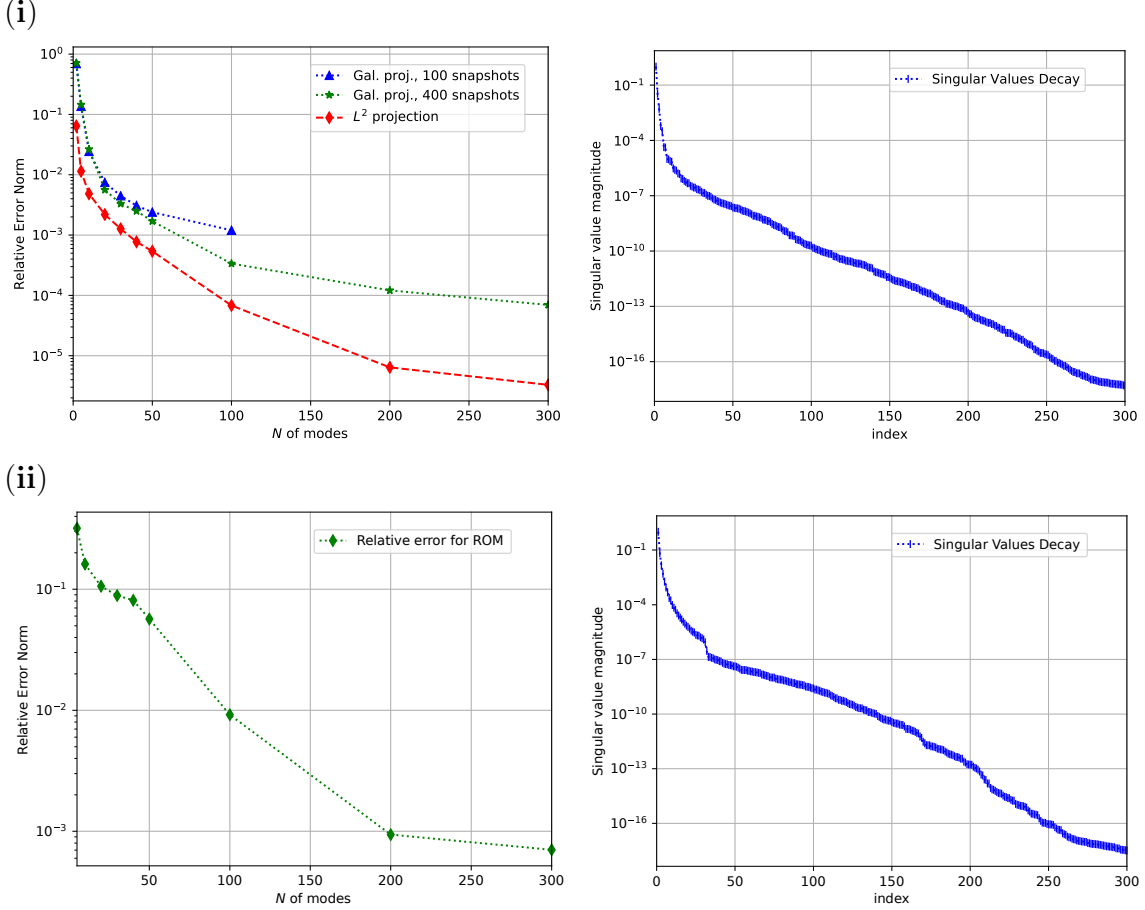


FIGURE 5. Heat exchange problem results for the first (i) and second (ii) numerical experiments. On the left we plot the mean relative error for the L^2 projection of the full order solution projected onto the POD basis functions (dashed red line with square markers) and the ROM solution for various number of modes (dotted blue and green lines with triangular and star markers). The error has been computed as the mean of the error of 50 snapshots using different parameter values with respect to those used to compute the POD modes. On the right, the singular value decay of the POD procedure is visualized.

4.2. Embedded rectangle with parametrized aspect ratio. In this test problem a fixed uniform source is applied over a rectangular \mathcal{D} using a parameter μ equal to the aspect ratio of the rectangle; the center of \mathcal{D} remains fixed within \mathcal{T} . The embedded domain consists of a rectangle of size $k_1 \times k_2$, for $k_1, k_2 \in \mathbb{R}$ and its size is parametrized by the parameter $\mu = \frac{k_1}{k_2}$ with the additional constraint given by $\mu k_2 = 0.2$. The ROM has been trained with 400 samples for $\mu \in [0.29, 6.67]$ chosen randomly inside the parameter space. To test the accuracy of the ROM we compared its results on 50 additional samples that were not used to create the ROM and were selected randomly within the same range. The background domain size is a square with dimensions $[-0.7, 0.7] \times [-0.7, 0.7]$ and it is discretized with mesh size $h = 0.035$.

To verify the behavior of the ROM and its sensitivity with respect to the number of modes in Figure 5 (ii) we compare, for different number of modes, the average of the L^2 norm relative error for the 50 different samples used to test the ROM. The plot is reported for the ROM results.

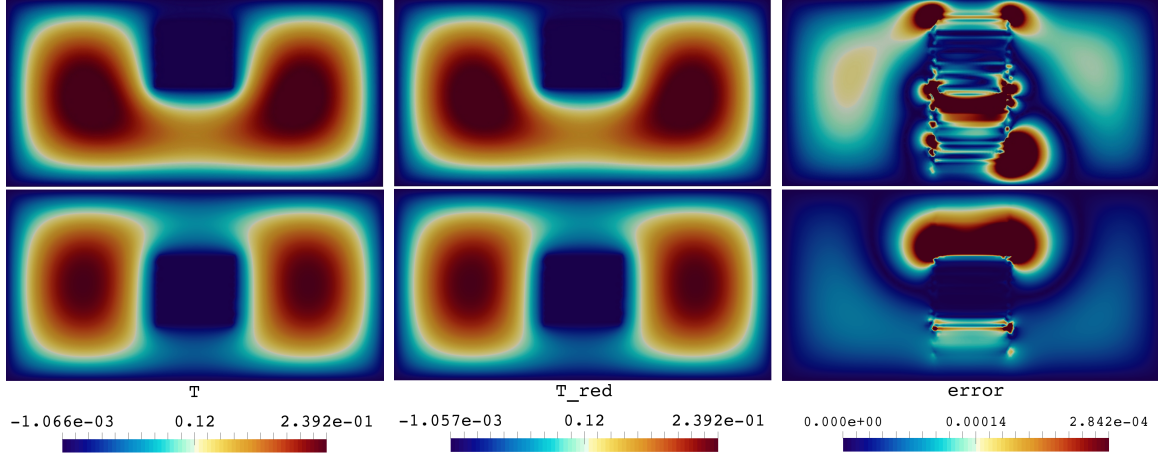


FIGURE 6. Heat exchange problem results for the first numerical example. From left to the right we report the full order solution, the reduced order solution and the absolute values of the error results respectively. The results are for two selected values of the parameter, $\mu = 0.403$ (first row) and $\mu = -0.015$ (second row).

TABLE 2. Execution time, savings and speed up using 400 snapshots in the online stage. The computation time includes the assembling of the full order matrices, their projection and the resolution of reduced problem. Results are reported for various dimensions of the reduced basis space.

Num of modes	Execution time(s) ^a	Savings ($t_{\text{FOM}} - t_{\text{RB}})/t_{\text{RB}}$ ^{b,c}	Speedup $t_{\text{FOM}}/t_{\text{RB}}$
2	4.119470×10^{-2}	96.399%	27.770
5	4.136089×10^{-2}	96.384%	27.658
10	4.168334×10^{-2}	96.356%	27.445
20	4.243647×10^{-2}	96.290%	26.957
30	4.353909×10^{-2}	96.194%	26.275
40	4.449359×10^{-2}	96.110%	25.711
50	4.494564×10^{-2}	96.071%	25.452
100	4.992923×10^{-2}	95.635%	22.912
200	6.156138×10^{-2}	94.618%	18.583
300	7.551091×10^{-2}	93.399%	15.150
FOM	1.14540×10^0	—	—

^a Online stage, ^b t_{FOM} is the FOM solution time, ^c t_{RB} is the RB solution time.

Some Comments. The plots of Figure 5 (ii) are generated with the ROM constructed using 400 snapshots. We are pointing out here that for both experiments, we observe a discrepancy between the convergence rate of the left and right side of Figure 5 (i) and (ii). The relative errors graph (left) shows a different convergence rate with respect to the eigenvalue decay. This happens because we compare the full order results obtained on a different training set respect to the one used to obtain the POD modes. In particular, we used the 50 different parameter values not previously used to train the ROM.

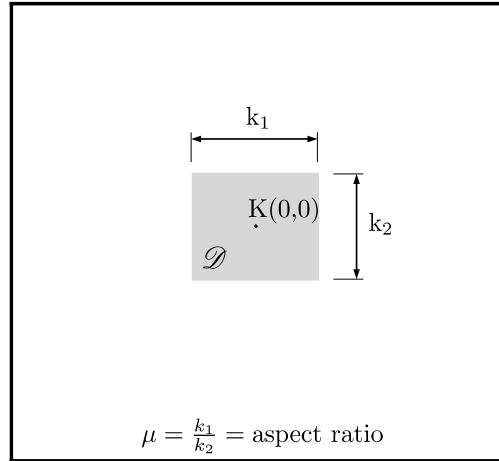


FIGURE 7. Background and embedded geometry for a rectangle with parameter its aspect ratio. $\mu = \frac{k_1}{k_2}$ and $\mu k_2 = 0.2$.

5. CONCLUSIONS AND FUTURE PERSPECTIVES

In this work we proposed a new reduced order modeling technique for parametrized geometries. We used an unfitted mesh finite element method to construct a reduced basis onto the background mesh which is independent with respect to the parameter and the parameterized geometry, applying a modified POD-Galerkin methodology. Such coupling, relying on a common background mesh permits to avoid some of the disadvantages related with a reference domain approach. The methodology has been tested on a simple geometrically parametrized heat transfer problem showing promising results. In terms of future perspectives, our interest is in testing the methodology on more complex scenarios and in particular on geometrically parametrized viscous flow problems governed by Stokes [15] and Navier-Stokes equations. Moreover our interest is also in investigating the efficiency of hyper reduction techniques to the proposed methodology in order to further increase the computational speedups and performances.

6. ACKNOWLEDGEMENT

We would like to thank the reviewers for their insightful comments on our work. This work is supported by the U.S. Department of Energy, Office of Science, Advanced Scientific Computing Research under Early Career Research Program Grant SC0012169, the U.S. Office of Naval Research under grant N00014-14-1-0311, ExxonMobil Upstream Research Company (Houston, TX), the European Research Council Executive Agency by means of the H2020 ERC Consolidator Grant project AROMA-CFD “Advanced Reduced Order Methods with Applications in Computational Fluid Dynamics” - GA 681447, (PI: Prof. G. Rozza), INdAM-GNCS 2018 and by project FSE European Social Fund HEaD “Higher Education and Development” SISSA operazione 1, Regione Autonoma Friuli-Venezia Giulia.

REFERENCES

- [1] Balajewicz, M.; Farhat, C.: Reduction of nonlinear embedded boundary models for problems with evolving interfaces. *Journal of Computational Physics*, Vol. 274, pp. 489–504, 2014.
- [2] Ballarin, F.; Manzoni, A.; Quarteroni, A.; Rozza, G.: Supremizer stabilization of POD-Galerkin approximation of parametrized steady incompressible Navier-Stokes equations. *International Journal for Numerical Methods in Engineering*, Vol. 102, No. 5, pp. 1136–1161, 2014.

- [3] Barrault, M.; Maday, Y.; Nguyen, N.; Patera: An 'empirical interpolation' method: application to efficient reduced-basis discretization of partial differential equations. *Comptes Rendus Mathematique*, Vol. 339, No. 9, pp. 667–672, 2004.
- [4] Benner, P.; Ohlberger, M.; Patera, A.; Rozza, G.; Urban, K.: *Model Reduction of Parametrized Systems*. No. Vol. 17 in MS&A series. Springer, 2017.
- [5] Carlberg, K.; Farhat, C.; Cortial, J.; Amsallem, D.: The GNAT method for nonlinear model reduction: Effective implementation and application to computational fluid dynamics and turbulent flows. *Journal of Computational Physics*, Vol. 242, pp. 623–647, 2013.
- [6] Chinesta, F.; Huerta, A.; Rozza, G.; Willcox, K.: *Model Order Reduction*. *Encyclopedia of Computational Mechanics*. Elsevier Editor, 2016.
- [7] Chinesta, F.; Ladeveze, P.; Cueto, E.: A Short Review on Model Order Reduction Based on Proper Generalized Decomposition. *Archives of Computational Methods in Engineering*, Vol. 18, No. 4, p. 395, 2011.
- [8] Dumon, A.; Allery, C.; Ammar, A.: Proper general decomposition (PGD) for the resolution of Navier–Stokes equations. *Journal of Computational Physics*, Vol. 230, No. 4, pp. 1387–1407, 2011.
- [9] Grepl, M.; Maday, Y.; Nguyen, N.; Patera, A.: Efficient reduced-basis treatment of nonaffine and nonlinear partial differential equations. *ESAIM: M2AN*, Vol. 41, No. 3, pp. 575–605, 2007.
- [10] Grepl, M.; Patera, A.: A posteriori error bounds for reduced-basis approximations of parametrized parabolic partial differential equations. *ESAIM: M2AN*, Vol. 39, No. 1, pp. 157–181, 2005.
- [11] Haasdonk, B.; Ohlberger, M.: Reduced basis method for finite volume approximations of parametrized linear evolution equations. *Mathematical Modelling and Numerical Analysis*, Vol. 42, No. 2, pp. 277–302, 2008.
- [12] Hesthaven, J.; Rozza, G.; Stamm, B.: *Certified Reduced Basis Methods for Parametrized Partial Differential Equations*. SpringerBriefs in Mathematics, 2016.
- [13] Kalashnikova, I.; Barone, M.F.: On the stability and convergence of a Galerkin reduced order model (ROM) of compressible flow with solid wall and far-field boundary treatment. *International Journal for Numerical Methods in Engineering*, Vol. 83, No. 10, pp. 1345–1375, 2010.
- [14] Karatzas, E.; Ballarin, F.; Rozza, G.: Projection-based reduced order models for a cut finite element method in parametrized domains. In preparation, 2018.
- [15] Karatzas, E.; Stabile, G.; Nouveau, L.; Rozza, G.; Scovazzi, G.: A Reduced Basis Approach for PDES on parametric geometry problem with the Shifted Boundary Finite Element Method and application to fluid dynamics. Submitted, 2018.
- [16] Kunisch, K.; Volkwein, S.: Galerkin proper orthogonal decomposition methods for a general equation in fluid dynamics. *SIAM Journal on Numerical Analysis*, Vol. 40, No. 2, pp. 492–515, 2002.
- [17] Main, A.; Scovazzi, G.: The shifted boundary method for embedded domain computations. Part I: Poisson and Stokes problems. *Journal of Computational Physics*, <https://doi.org/10.1016/j.jcp.2017.10.026>, in press, 2017.
- [18] Main, A.; Scovazzi, G.: The shifted boundary method for embedded domain computations. Part II: Linear advection-diffusion and incompressible Navier-Stokes equations. *Journal of Computational Physics*, <https://doi.org/10.1016/j.jcp.2018.01.023>, in press, 2018.
- [19] Quarteroni, A.; Manzoni, A.; Negri, F.: *Reduced Basis Methods for Partial Differential Equations*. Springer International Publishing, 2016.
- [20] Rozza, G.: Reduced basis methods for Stokes equations in domains with non-affine parameter dependence. *Computing and Visualization in Science*, Vol. 12, No. 1, pp. 23–35, 2009.
- [21] Rozza, G.; Huynh, D.; Patera, A.: Reduced basis approximation and a posteriori error estimation for affinely parametrized elliptic coercive partial differential equations: Application to transport and continuum mechanics. *Archives of Computational Methods in Engineering*, Vol. 15, No. 3, pp. 229–275, 2008.
- [22] Rozza, G.; Huynh, D.B.P.; Manzoni, A.: Reduced basis approximation and a posteriori error estimation for Stokes flows in parametrized geometries: roles of the inf-sup stability constants. *Numerische Mathematik*, Vol. 125, No. 1, pp. 115–152, 2013.
- [23] Rozza, G.; Veroy, K.: On the stability of the reduced basis method for Stokes equations in parametrized domains. *Computer Methods in Applied Mechanics and Engineering*, Vol. 196, No. 7, pp. 1244–1260, 2007.

- [24] Sirovich, L.: Turbulence and the Dynamics of Coherent Structures part I: Coherent Structures. *Quarterly of Applied Mathematics*, Vol. 45, No. 3, pp. 561–571, 1987.
- [25] Song, T.; Main, A.; Scovazzi, G.; Ricchiuto, M.: The shifted boundary method for hyperbolic systems: Embedded domain computations of linear waves and shallow water flows. *Journal of Computational Physics*, Vol. 369, pp. 45–79, 2018.
- [26] Veroy, K.; Prud’homme, C.; Patera, A.: Reduced-basis approximation of the viscous Burgers equation: rigorous a posteriori error bounds. *Comptes Rendus Mathematique*, Vol. 337, No. 9, pp. 619–624, 2003.
- [27] Xiao, D.; Fang, F.; Buchan, A.; Pain, C.; Navon, I.; Du, J.; Hu, G.: Non linear model reduction for the Navier–Stokes equations using residual DEIM method. *Journal of Computational Physics*, Vol. 263, pp. 1–18, 2014.